

Dynamical analysis of low-energy-electron-diffraction intensities from GaP(110)

C. B. Duke, A. Paton, and W. K. Ford

Xerox Webster Research Center, Xerox Square-114, Rochester, New York 14644

A. Kahn and J. Carelli

Department of Electrical Engineering, Princeton University, Princeton, New Jersey 08540

(Received 23 February 1981)

An analysis of the structure of the (110) surface of GaP is performed by comparing dynamical calculations of elastic low-energy electron diffraction (ELEED) intensities with those measured at $T = 300$ K. Prior analyses of ELEED intensities from compound semiconductor surfaces are extended by considering both energy-independent (Slater) and energy-dependent (Hara) models of the exchange potential and by utilizing R -factor methods to assess the quality of the description of the measured intensities by the calculated ones. A description of the measured intensities is achieved which is as good as the best obtained earlier for analogous surfaces of other compound semiconductors: i.e., GaAs(110), InSb(110), InP(110), and ZnTe(110). The resulting best-fit structures consist of single-layer reconstructions characterized by a rotation angle of $\omega_1 = 25^\circ \pm 3^\circ$ and a relaxation of the rotated top layer toward the substrate by 0.1 ± 0.05 Å. The top layer reconstruction is essentially identical to that for GaAs(110) and InSb(110), but relaxed 0.05 Å closer to the substrate. In contrast to these two surfaces, however, no evidence is obtained for second-layer reconstructions on GaP(110), a result which may be due to the fact that the ELEED intensity data for GaP(110) were acquired at $T = 300$ K, whereas those for GaAs(110) and InSb(110) were obtained at $T = 150$ K.

I. INTRODUCTION

In a previous series of papers we have analyzed measured elastic low-energy electron diffraction (ELEED) intensities to determine the surface atomic geometries of GaAs(110),^{1,2} InSb(110),^{3,4} InP(110),^{5,6} and ZnTe(110).^{7,8} The purpose of this paper is to extend these analyses to GaP(110).

Our structure analysis consists of comparing ELEED intensities calculated using multilayer multiple-scattering programs, described elsewhere,^{2,9} with those measured from ion-bombarded and annealed GaP(110) at room temperature. The procedure utilized for determining the surface structure is that of minimizing the x-ray R factor, R_x , as discussed in our earlier study of InP(110).⁶ Herein, we extend and evaluate this procedure in three important respects. First, we assess the influence of the reproducibility of the ELEED intensity measurements on the predicted R factors. Second, we examine the consequences of two of the most important nonstructural parameters, the electron exchange potential⁹ and the inelastic collision mean free path,^{6,10} on the values of the R factors obtained for a given set of data. The other important nonstruc-

tural parameter, the real part of the inner potential,¹⁰ is determined during the R -factor analysis procedure.⁶ Third, we determine the influence of thermal lattice vibrations^{11,12} on the R factors and structures emanating from the analysis.

Our major result is that independent of the uncertainties introduced by the nonstructural parameters and lattice vibrations, GaP(110) is reconstructed in a fashion analogous to but not identical with InP(110).^{5,6} The top layer is characterized by a bond-length-conserving rotation of $\omega_1 = 25^\circ \pm 3^\circ$ and a contraction by 0.1 ± 0.05 Å toward the substrate. The definition of the quantities specifying the surface structure is given in Fig. 1 using the bulk structure parameters specified in Wyckoff.¹³ There is no evidence for second-layer distortions for GaP(110), in contrast to GaAs(110) and InSb(110) for which the evidence for these distortions is strong¹⁻⁴ but analogous to InP(110) for which the evidence for them is weak.⁶ This result could be significant in discerning relationships between surface structure and the nature of the bulk chemical bonding in tetrahedrally coordinated compound semiconductors because using Phillip's scale¹⁴ GaP exhibits a spectroscopic ionicity of $f_i = 0.37$, intermediate between GaAs

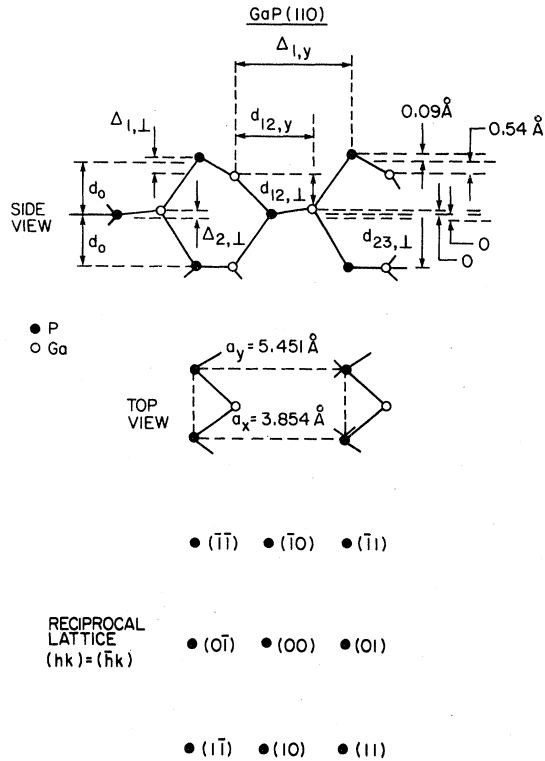


FIG. 1. Schematic indication of the surface atomic geometry and the associated ELEED normal incidence spot pattern for the (110) surface of GaP. The symbols utilized in Table I are defined in the upper panel of the figure. The numerical values are taken from row (d) of Table I.

($f_i = 0.31$) and InSb ($f_i = 0.32$) on the one hand and InP ($f_i = 0.42$) on the other. Using the Pauling scales, however, the order of GaP and InP is reversed, i.e., $f_i(\text{InSb}) < f_i(\text{GaAs}) = f_i(\text{InP}) < f_i(\text{GaP})$, so the GaP exhibits an ionicity intermediate between those of InP and of ZnTe.¹⁴ Alternatively, since the GaP ELEED intensity data were taken at $T = 300$ K, whereas the data for GaAs, InSb, and InP were acquired at $T = 150$ K, the absence of second-layer distortions for GaP(110) may be a thermal effect reflecting the disappearance of these distortions for GaP with increasing temperature.

We proceed by indicating the experimental procedures in Sec. II and the calculational ones in Sec. III. A discussion of the sensitivity of the calculated R factors to the use of different data sets and to the values of the nonstructural parameters is given in Sec. IV. We present the final results of our structure analysis for GaP(110) in Sec. V and conclude with a synopsis of our major conclusions.

II. EXPERIMENTAL PROCEDURES

Measurements of the ELEED intensities from GaP(110) were performed in two standard ultra-high vacuum LEED/Auger systems, one from Varian Associates (VA), the second from Physical Electronics (PE). Each consists of a four grid LEED optics with a phosphor screen display (VA) #981-0127, PE #15-120 and a 3-kV cylindrical mirror analyzer (VA #981-2707, PE 15-100). LEED intensities, measured using a telescopic spot photometer (Gamma Scientific #2009), were subsequently corrected for variations in primary beam current and background. Energy-intensity profiles were taken at normal electron beam incidence. The plane of incidence was assured by determining that symmetrically equivalent beams provided the same profiles to within a few percent. Normal incidence was verified by the alignment of the spot pattern. Since this procedure is only accurate to within a few degrees, sample alignment is probably the major source of uncertainty in the intensity data.

GaP crystals were polished courtesy of RCA laboratories to achieve mirror smooth (110) surfaces. Each crystal was then mounted in a molybdenum foil envelope on a rotatable, temperature controlled manipulator. After insertion into the vacuum chamber, the surface was bombarded by 1-kV argon ions for 20 min. This provided a clean surface showing only lattice constituents in the electron stimulated Auger spectrum to the limit of the analyzer resolution. The surface was then annealed for 4 h at 550°C, a procedure which yielded a high-quality LEED pattern. LEED intensities were measured using two separate GaP samples, one inserted in each of the two systems described above. Reproducibility was good, between both samples and experimental systems, as will be discussed further in Sec. IV A.

An initial set of ELEED profiles was obtained for 14 beams, (01) , $(11) = (\bar{1}\bar{1})$, $(10) = (\bar{1}0)$, $(1\bar{1}) = (\bar{1}\bar{1})$, $(0\bar{1})$, (02) , $(12) = (\bar{1}\bar{2})$, $(21) = (\bar{2}\bar{1})$, $(20) = (\bar{2}0)$, $(2\bar{1}) = (\bar{2}\bar{1})$, $(1\bar{2}) = (\bar{1}\bar{2})$, $(0\bar{2})$, $(13) = (\bar{1}\bar{3})$, and $(\bar{1}3) = (\bar{1}\bar{3})$, at three-volt increments in primary voltage. A second set of profiles was measured using another crystal in a second system. Intensity profiles were measured for the pairs of beams listed above with each pair averaged together, giving 10 different averaged intensity profiles. The remaining four beams, those with no symmetric counterparts, were taken twice and averaged to yield a complete set of intensity profiles for the same 14 beams considered in the initial experiments. Intensities in this second set were measured at 2-eV incre-

ments. These profiles agreed well with the initial data. The combination of these two sets of measured intensity profiles constitutes the raw data used in our assessment of the consequences of the reproducibility of the experimental measurements on the ELEED structure analysis. The second set of data was used as the basis for our structure analysis.

III. MODEL CALCULATIONS

An approximate multiple-scattering model of the diffraction process, described previously,² was used to perform our dynamical calculations of the ELEED intensities. In this model, which is embodied in a series of computer programs, the scattering species are represented by energy-dependent phase shifts in terms of which the ELEED intensities from the surface are computed. The scattering amplitudes associated with the uppermost three atomic bilayers are evaluated exactly, as are those of each of the individual atomic layers beneath. The interference between the upper three layers and the various layers in the substrate is calculated as described by Meyer *et al.*² The accuracy of this approximation has been verified in the analysis of another zinc blende (110) surface, that of ZnTe(110), where the intensity profiles calculated solving the scattering in the uppermost four atomic bilayers exactly were compared with those calculated solving the scattering in the uppermost three bilayers exactly.⁸ Convergence tests revealed that the consideration of a slab of six atomic layers and the use of six phase shifts for each scatterer yield predicted intensities which are generally accurate to within a few percent, so these parameters were adopted for the calculations presented herein.

The electron-ion core interaction is described by a one-electron muffin-tin potential. The one-electron crystal potential is formed from a superposition of overlapping ionic (e.g., Ga^+P^-) charge densities. Two models of the exchange interaction were used to obtain the crystal potential from these charge densities: (energy-independent) Slater exchange^{15,16} and (energy-dependent) Hara exchange.^{9,17} A discussion of the comparison of these models with others used in ELEED intensity calculations is given elsewhere.^{6,9} The bulk crystal structure (see Fig. 1) is that given by Wyckoff.¹³ We use the muffin-tin radii $r_{\text{MT}}(\text{Ga}) = 1.17 \text{ \AA}$, $r_{\text{MT}}(\text{P}) = 1.19 \text{ \AA}$, for the Slater-exchange potential and $r_{\text{MT}}(\text{Ga}) = 1.10 \text{ \AA}$, $r_{\text{MT}}(\text{P}) = 1.26 \text{ \AA}$ for the Hara-exchange potential as determined from crystal potential crossover. The

Wigner-Seitz radii are $r_{\text{WS}}(\text{Ga}) = 1.67 \text{ \AA}$ and $r_{\text{WS}}(\text{P}) = 1.70 \text{ \AA}$. Once the crystal potential in a given Wigner-Seitz cell has been obtained, the potential is reduced to muffin-tin form as described by Duke *et al.*,¹⁵ for Slater exchange and by Meyer *et al.*⁹ for Hara exchange. The phase shifts resulting from these two potentials are shown in Figs. 2 and 3, respectively. The differences between the two sets of phase shifts are analogous to those reported earlier for GaAs:⁹ The $l = 0$ and $l = 1$ phase shifts tend to increase, the others tend to increase, the others tend to decrease, and the $l = 2$ phase shift for Ga exhibits a qualitative change in behavior in both cases.

The electron-electron interaction is incorporated via a complex inner potential¹⁰ with a constant real part V_0 and an imaginary part characterized by the inelastic collision mean free path λ_{ee} .¹⁸ We selected V_0 to minimize either the Zanazzi-Jona R factor¹⁹ [given by Eqs. (7)–(14) and (16) of Ref. 19] or the x-ray R factor [given by Eqs. (3), (8), (13), (14), and (16) of Ref. 19]. Our major structure searches were performed using $\lambda_{ee} = 8 \text{ \AA}$, although we examined the sensitivity of the values of both R factors to the

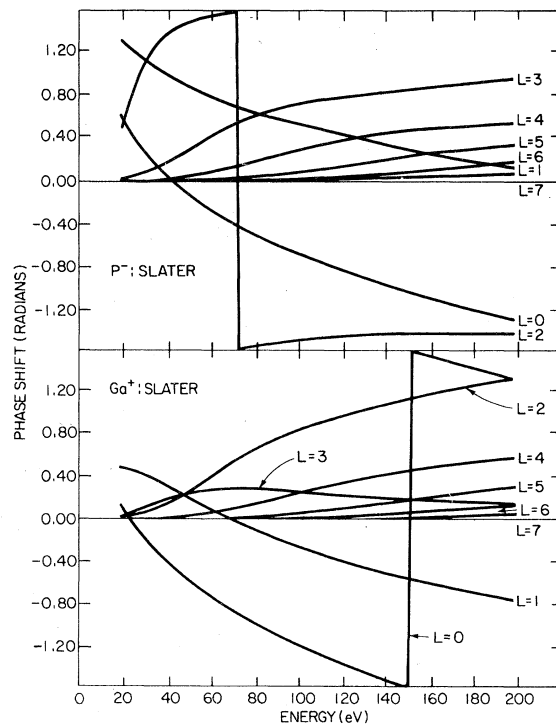


FIG. 2. Phase shifts for the Ga^+ and P^- species resulting from Slater exchange, using $r_{\text{MT}}(\text{P}) = 1.19 \text{ \AA}$, $r_{\text{MT}}(\text{Ga}) = 1.17 \text{ \AA}$, $r_{\text{WS}}(\text{Ga}) = 1.67 \text{ \AA}$, and $r_{\text{WS}}(\text{P}) = 1.70 \text{ \AA}$.

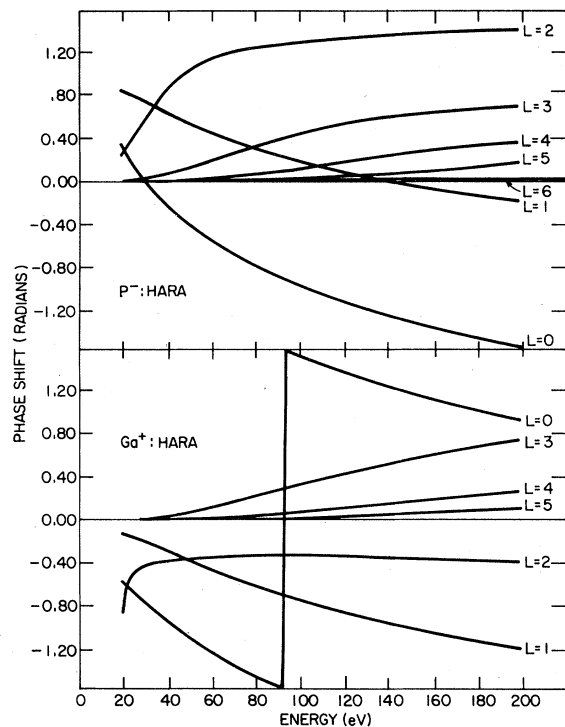


FIG. 3. Phase shifts for the Ga^+ and P^- species resulting from Hara exchange, using the radii $r_{\text{MT}}(\text{P}) = 1.26 \text{ \AA}$ and $r_{\text{MT}}(\text{Ga}) = 1.10 \text{ \AA}$. The Wigner-Seitz radii are not used in the calculation of the Hara potential (Ref. 9).

value of λ_{ee} as discussed below.

The consequences of thermal lattice vibrations are neglected in the structure search reported herein, which are performed for a rigid lattice of scatterers. We did, however, investigate the effect of including the consequences of the *bulk* lattice vibrations on the calculated intensities *a posteriori*, for the unreconstructed and x-ray *R*-factor “best-fit” structures. The vibrational amplitudes were taken from the x-ray measurements of Shumskii *et al.*¹¹ They are incorporated in the model via use of Eqs. (39)–(51) of Jepsen *et al.*,²⁰ to calculate complex phase shifts, but utilizing for each atomic species

$$A = (u_0^2 + cT)/6 \quad (1)$$

in lieu of Eq. (44) in Ref. 20. Specifically, we used $u_0^2(\text{P}) = 5.5 \times 10^{-3} \text{ \AA}^2$, $u_0^2(\text{Ga}) = 0$, $c(\text{P}) = 7.72 \times 10^{-5} \text{ \AA}^2/\text{K}$, and $c(\text{Ga}) = 7.58 \times 10^{-5} \text{ \AA}^2/\text{K}$ obtained from fitting Eq. (1) to the results shown in Fig. 2 of Ref. 11. As expected on the basis of our previous experience with GaAs(110),² inclusion of the bulk lattice vibrations in the model reduced the calculated ELED intensities fairly uniformly by a factor of about 2. Since we did not acquire mea-

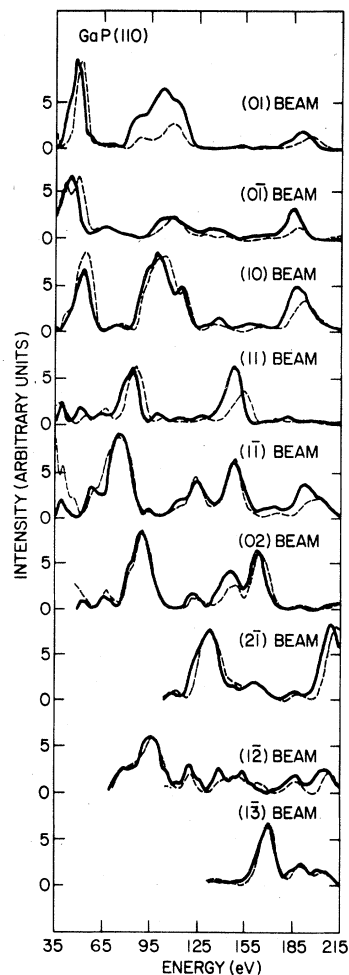


FIG. 4. Comparison of two independent sets of measured ELED intensities for electrons normally incident on GaP(110) at room temperature. The beams shown are those for which the full structure analysis of GaP(110) is illustrated in Figs. 6–14. Different GaP crystals and different LEED instruments were used to obtain the two sets of intensity profiles.

sured ELED intensities at a variety of temperatures, an assessment of the relative magnitudes of the surface and bulk vibrational amplitudes was not possible.

IV. SENSITIVITY ANALYSIS

A. Data reproducibility

One of our first observations in utilizing *R*-factor programs was that when we analyzed different sets of nominally equivalent ELED intensity data, the values of R_x but more especially R_{ZJ} could vary widely (i.e., up to factors of 2) when a given calcula-

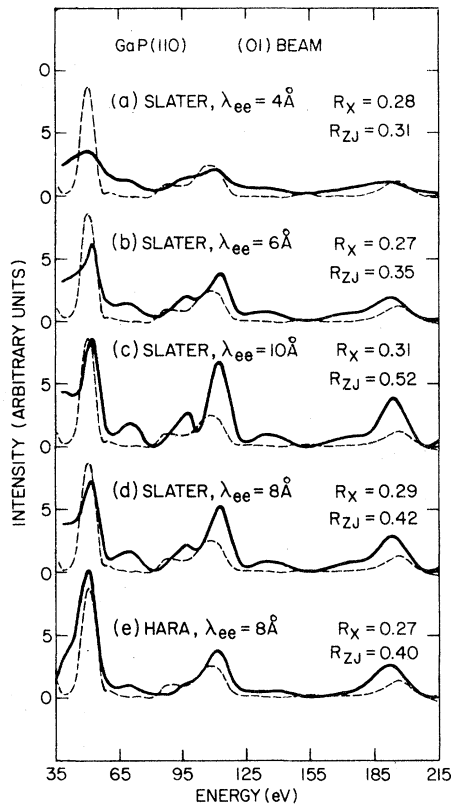


FIG. 5. Comparison of the intensity profiles predicted for the unreconstructed surface structure of GaP(110) (solid lines) with the measured intensities (dashed lines) for normally incident electrons diffracted into the (01) beam. (a) Slater exchange, $\lambda_{ee} = 4 \text{ \AA}$, $V_0 = 14 \text{ eV}$, $R_x = 0.28$, $R_{ZJ} = 0.31$. (b) Slater exchange, $\lambda_{ee} = 6 \text{ \AA}$, $V_0 = 14 \text{ eV}$, $R_x = 0.27$, $R_{ZJ} = 0.35$. (c) Slater exchange, $\lambda_{ee} = 10 \text{ \AA}$, $V_0 = 14 \text{ eV}$, $R_x = 0.31$, $R_{ZJ} = 0.52$. (d) Slater exchange, $\lambda_{ee} = 8 \text{ \AA}$, $V_0 = 14 \text{ eV}$, $R_x = 0.29$, $R_{ZJ} = 0.42$. (e) Hara exchange, $\lambda_{ee} = 8 \text{ \AA}$, $V_0 = 15 \text{ eV}$, $R_x = 0.27$, $R_{ZJ} = 0.40$. All calculations were performed for a rigid lattice.

tion was compared to nominally equivalent but independently acquired sets of data. Our intent in this section is to document these observations and place them in perspective.

First, to illustrate the reproducibility of our measured ELED intensities from GaP(110) we show in Fig. 4 the comparison of nine intensity profiles obtained using both different crystals and different LEED instruments as described in Sec. II. It is evident that the reproducibility of the major features in these data is excellent, although there is some variation in the shape and absolute magnitude of certain of these features between the two independent experiments. Some of these variations, e.g., the shifts in the peaks near 190 eV in the (01), (0 $\bar{1}$), and (10)

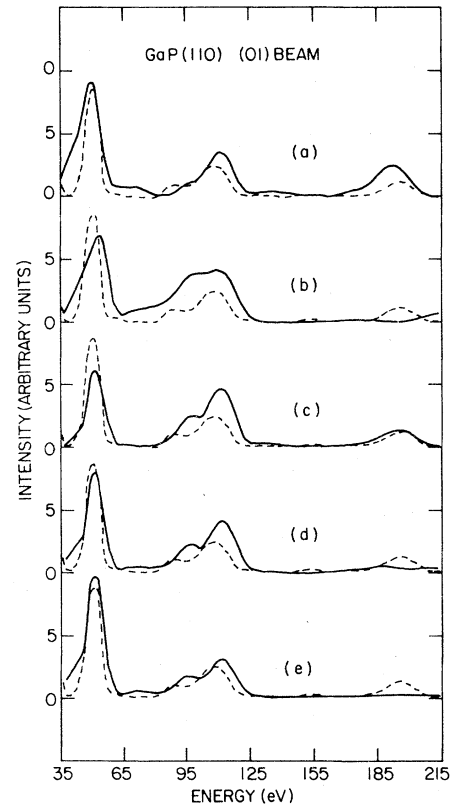
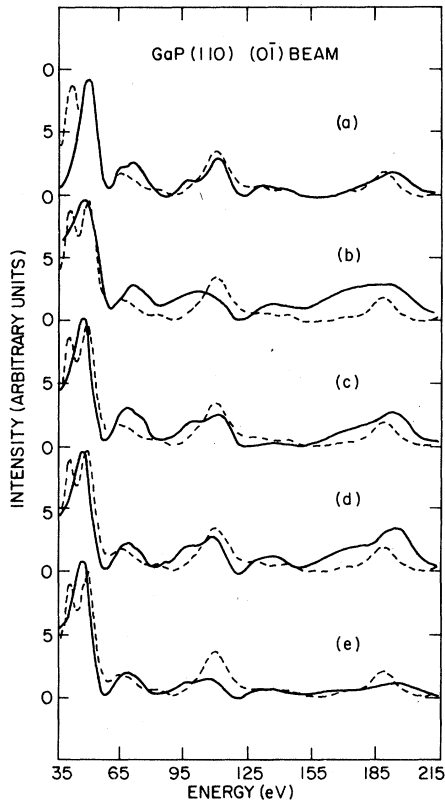
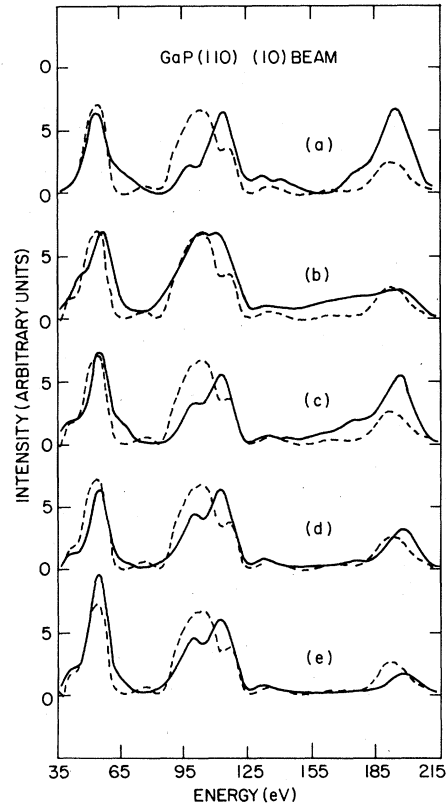


FIG. 6. Comparison of calculated (solid lines) and measured (dashed lines) intensities of electrons normally incident on GaP(110) diffracted into the (01) beam. (a) Calculated intensities for the unreconstructed surface structure as specified in row (a) of Table I evaluated for a rigid lattice. (b) Calculated intensities for the structure that minimizes the Zanazzi-Jona R factor as specified in row (c) of Table I evaluated for a rigid lattice. (c) Calculated intensities for the structure that provides the best visual fit to the data as specified in row (e) of Table I evaluated for a rigid lattice. (d) Calculated intensities for the structure that minimizes the x-ray R factor as specified in row (d) of Table I evaluated for a rigid lattice. (e) Same as (d) but evaluated for a vibrating lattice at $T = 300 \text{ K}$.

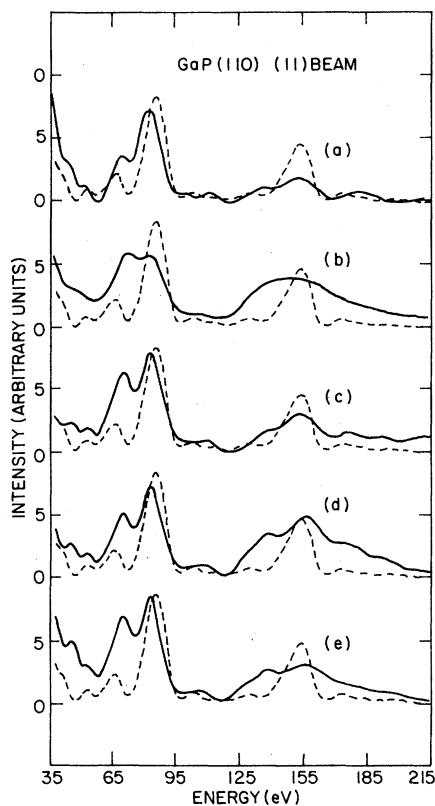
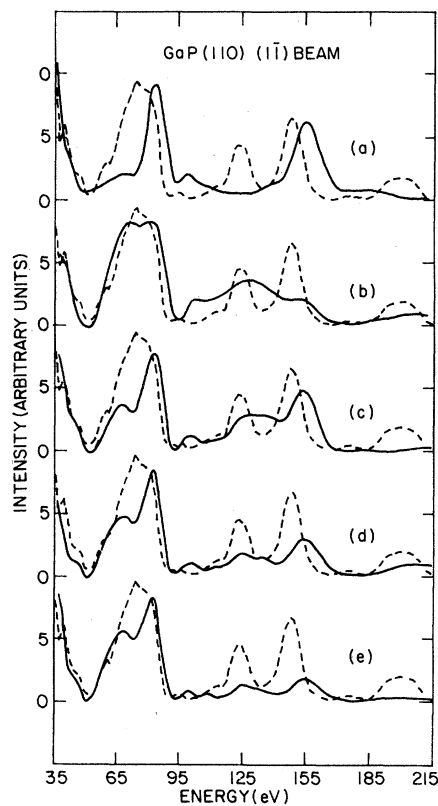
beams or the lineshape change near 90 eV in the (11) beam, lead to quite discernable differences in the R factors obtained when comparing calculated intensities to these data. We believe this figure illustrates the reproducibility to be expected from one laboratory to another because of our use of totally different samples and instruments in the two cases. Uncertainties in sample alignment as well as variations in surface preparation, phosphor uniformity on the LEED screen, background normalization, and spot photometer calibration all contribute to the difference between these two sets of data. Neverthe-

FIG. 7. Same as Fig. 6 for the $(0\bar{1})$ beam.FIG. 8. Same as Fig. 6 for the $(10) = (\bar{1}0)$ beam.

less, these data are equally if not more reproducible than those published for other semiconductor surfaces, e.g., Si(100)-(2 × 1).²¹ Therefore we believe that these data are representative of the state of the art for semiconductor surfaces at the present time.

We can estimate the *accuracy* (as opposed to the *precision*) of R -factor methods applied to these data by utilizing one set of data (the averaged data taken at 2-eV intervals as described in Sec. II) as "data" to be compared with the other as "theory." Doing this we find $R_x = 0.10$ and $R_{ZJ} = 0.25$ for our two sets of 14 intensity profiles, 9 of which are shown in Fig. 4. For comparison, if we use our low temperature GaAs(110) data^{1,2} as theory we find $R_x = 0.51$ and $R_{ZJ} = 0.44$, clearly unacceptable values of these quantities.¹⁹ Yet if we compare room temperature ZnS(110) data²² with the GaP(110) 2-eV interval data we obtain $R_x = 0.16$ and $R_{ZJ} = 0.27$. Thus, using the Zanazzi-Jona R factor as the comparison criterion, ZnS(110) is as similar to GaP(110) as two independent sets of GaP(110) data are to each other. The x-ray R factor also suggests that the data from these materials are very similar, as might be expected, given their nearly equal lattice constants and the locations of Zn, Ga, P, and S in the periodic table.

No global conclusions are warranted on the basis of these results since they are representative only of our own sample-preparation and data-acquisition procedures on compound semiconductor surfaces.¹⁻⁸ The results suggest to us, however, that it is unreasonable to expect values of R_x below about 0.1 and values of R_{ZJ} below about 0.3 for model calculation "fits" to the data for GaP(110), and that R_x is likely to be a more discriminating measure of the quality of the fit than R_{ZJ} . Using these criteria our model calculations described in subsequent sections are as good as can be expected on the basis of R_{ZJ} but in principle could be improved on the basis of R_x if the *electron-solid interaction and the sample alignment were known exactly*. Typically, structures in the vicinity of the best-fit structure [rows (c)–(e) in Table I] exhibit R factors in the ranges $0.17 \leq R_x \leq 0.20$, $0.27 \leq R_{ZJ} \leq 0.31$ for the averaged 2-eV-interval data and in the range $0.16 \leq R_x \leq 0.20$, $0.22 \leq R_{ZJ} \leq 0.25$ for the earlier 3-eV-interval data. For a given structure close to the optimal ones, the 3-eV-interval data typically yield values of R_x lower by 0.01 and values of R_{ZJ} lower by 0.05 than the 2-eV averaged data, although *both sets of data lead to the same optimal structures*. For

FIG. 9. Same as Fig. 6 for the $(11) = (\bar{1}\bar{1})$ beam.FIG. 10. Same as Fig. 6 for the $(1\bar{1}) = (\bar{1}\bar{1})$ beam.

the remainder of the paper we quote R values only for the 2-eV-interval data. These are the data which we show in Figs. 5–14.

B. Nonstructural parameters

Another source of uncertainty in model calculations of experimental ELED intensities is the fact that the electron-solid interaction is known imprecisely and described by approximate models.¹⁰ This fact will cause additional discrepancies between the calculated and measured intensities which will manifest themselves as increases in the R factors. Our purpose in this section is to estimate these increases for the model embodied in our computations of ELED intensities from tetrahedrally coordinated compound semiconductors, GaP(110) in particular.

The nonstructural parameters embodied in our model are those characteristic of the overlapping ionic (atomic) potential used to calculate the electron-ion-core phase shifts (see Figs. 2 and 3) and the two inner potential parameters, V_0 and λ_{ee} (see Sec. III). We obtain one value of V_0 for each model calculation by minimizing the x-ray or the Zanazzi-Jona R factor averaged over all 14 beams. Thus, the values of V_0 obtained by minimizing R_x

are given in Table I for our final candidate structures. Other procedures are possible. For example Shih *et al.*²³ minimize both V_0 and the structure parameters for each beam individually in their analysis of Fe(110). Although we can obtain smaller R factors by varying V_0 individually for each beam, we did not adopt this procedure because the physical model of the ELED process requires that once the incident beam parameters and the structural model are fixed, the inner potential should be the same for all of the diffracted beams.¹⁰

The values of the R factors also are sensitive to the choice of λ_{ee} as noted earlier⁶ for InP(110). Typically, for a given structural model R_{ZJ} is minimized by small values of $4 < \lambda_{ee} < 6 \text{ \AA}$, whereas R_x exhibits minima at somewhat larger values, e.g., $6 < \lambda_{ee} < 8 \text{ \AA}$. This result is illustrated in Fig. 5 for the unreconstructed surface structure and the (01) beam. The R factors averaged over all 14 beams also are specified in the figure to provide an index of the overall quality of the description of the measured intensities. From calculations like these for various structures we find that variations in R_x of $\Delta R_x \sim 0.02$ and in R_{ZJ} of $\Delta R_{ZJ} \sim 0.1$ can result for a given structure from nonoptimal models

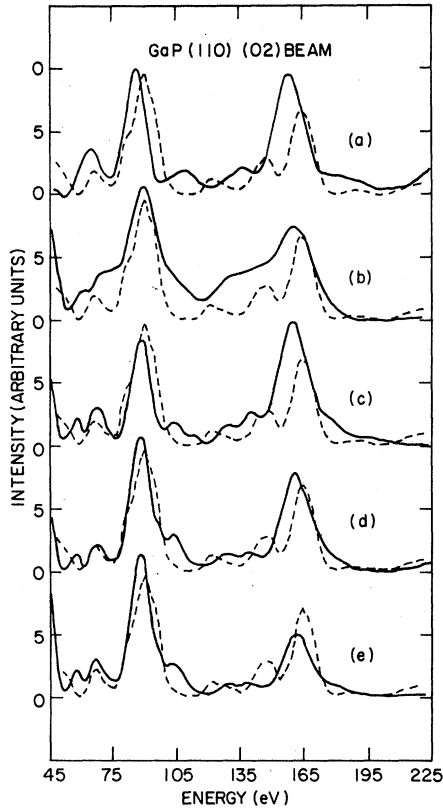
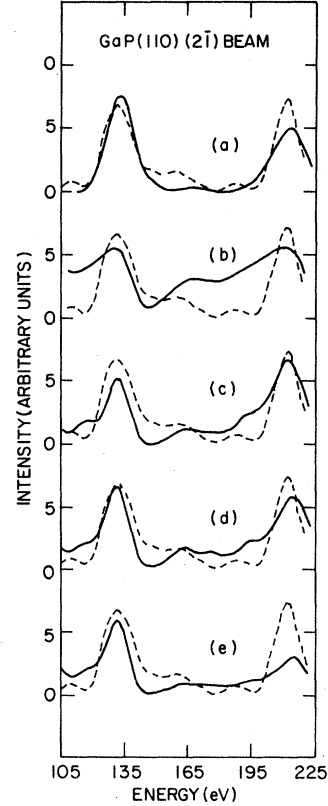


FIG. 11. Same as Fig. 6 for the (02) beam.

of the imaginary part of the inner potential.

Several parameters are involved in the construction of the model of the electron-ion-core scattering factors, including the muffin-tin radii, the value of the potential outside these radii, and the model of the exchange interaction.^{9,10,15} Since Meyer, Duke, and Paton⁹ found that the use of an energy-dependent (Hara) exchange improved significantly the model description of ELEED from GaAs(110), we have incorporated their model into our standard intensity calculation. The consequences of replacing energy-independent Slater exchange with energy-dependent Hara exchange are illustrated in Figs. 5(d) and 5(e) for an unreconstructed surface geometry. Evidently the use of Hara exchange improves the description of the measured intensities by this geometry by $\Delta R_x = 0.02$ and $\Delta R_{ZJ} = 0.02$, a result which is typical more generally for surface geometries in the vicinity of the best-fit structure, although the improvement is a little greater there ($\Delta R \sim 0.03$). Since the potentials associated with these models of exchange are constructed somewhat differently,^{9,15} we estimate that $\Delta R < 0.03$ is a

FIG. 12. Same as Fig. 6 for the $(2\bar{1}) = (\bar{2}1)$ beam.

reasonable uncertainty in the values of R associated with the choice of electron-ion-core potential.

Combining the results for λ_{ee} and the electron-ion-core potential, we arrive at the estimated root-mean-square uncertainties

$$\Delta R_x(\text{theor}) \simeq [(0.02)^2 + (0.03)^2]^{1/2} = 0.04, \quad (1a)$$

$$\Delta R_{ZJ}(\text{theor}) \simeq [(0.1)^2 + (0.03)^2]^{1/2} = 0.1, \quad (1b)$$

associated with the construction of model electron-solid force laws for a fixed (optimal) value of V_0 for all of the diffracted beams at fixed incident beam angles and for a given model structure. Compared with those associated with data reproducibility as estimated in Sec. IV A, i.e., $\Delta R_x(\text{expt}) = 0.1$, $\Delta R_{ZJ}(\text{expt}) = 0.3$, the theoretical uncertainties given in Eq. (1) are modest. The total root-mean-square uncertainties are

$$\Delta R_x(\text{abs}) = [\Delta R_x^2(\text{theor}) + \Delta R_x^2(\text{expt})]^{1/2} = 0.11, \quad (2a)$$

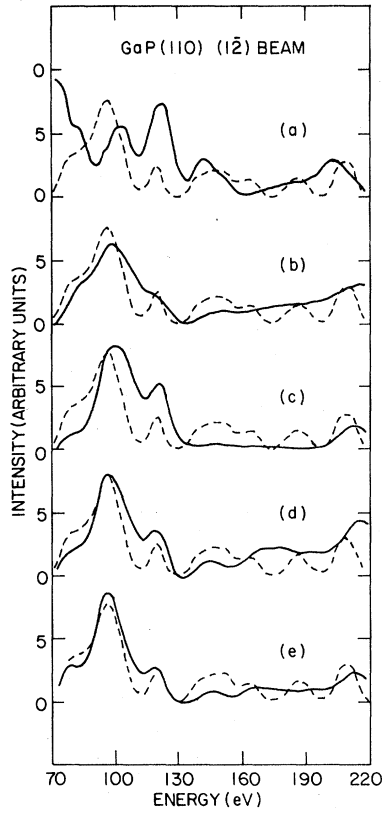


FIG. 13. Same as Fig. 6 for the $(\bar{1}\bar{2}) = (\bar{1}\bar{2})$ beam.

$$\begin{aligned} \Delta R_{ZJ}(\text{abs}) &= [\Delta R_{ZJ}^2(\text{theor}) + \Delta R_{ZJ}^2(\text{expt})]^{1/2} \\ &= 0.32 \end{aligned} \quad (2b)$$

These numbers provide an indication of the accuracy of the *absolute magnitude* of the R factors for a given surface structure. They do *not* provide an estimate of the uncertainties in these quantities associated with various surface structures for a given set of data and given model force law. Such estimates must be made by using different optimization criteria and assessing the comparative results. We carried out this procedure for InP(110) earlier⁶ and have repeated it for GaP(110) [see rows (c)–(e) in Table I]. For comparative purposes, therefore, we find

$$\Delta R_x(\text{fixed model}) = 0.04 \quad (3a)$$

$$\Delta R_{ZJ}(\text{fixed model}) = 0.08 \quad (3b)$$

as the *upper limits* of changes in the R factors which are significant to ensure discrimination between various structures. Because Eqs. (3) are upper limits, they are weak criteria which, however, ensure struc-

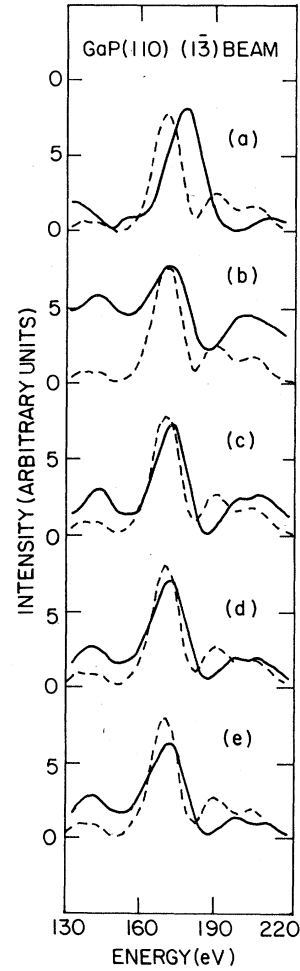


FIG. 14. Same as Fig. 6 for the $(\bar{1}\bar{3}) = (\bar{1}\bar{3})$ beam.

tural discrimination. Thus, from Table I we obtain the powerful result that in spite of good visual fits to several beams, neither the unreconstructed [row (a)] nor the Miller-Haneman [row (b)] structures lead to acceptable descriptions of ELED from GaP(110) because both violate the upper limit specified by Eq. (3a).

V. STRUCTURE ANALYSIS

Our structure analysis consisted of selecting five starting structures and making systematic variations of the structural parameters around each in order to find local minima in values of R_x and R_{ZJ} . Our starting structures were the unreconstructed surface of GaP(110),¹³ the structures of GaAs(110)^{1,2} and InP(110)⁶ scaled to the lattice constant of GaP, the energy-minimized structure proposed by Miller and

Haneman,²⁴ and a kinematically determined starting structure consisting of atomic relaxations normal to the surface penetrating three layers into the surface. Only one clear minimum in R_x was identified by this procedure. It occurs in the vicinity of bond-rotated top-layer reconstructions characterized by rotation angles of $\omega \sim 27^\circ$ and contractions toward the substrate of about 0.1 Å. The three structures in the vicinity of this minimum which minimize R_{ZJ} , minimize R_x , and give what we consider to be the best visual fit are specified in rows (c)–(e), respectively, of Table I. The description of the intensity profiles shown in Fig. 4 afforded by all three of these structures as well as by the unreconstructed surface geometry is shown in Figs. 6–14. We also examined the top-layer-contraction-by-0.1 Å structure proposed by Lee *et al.*²⁵ and found that it yielded a quite unsatisfactory description of our intensity data characterized by $R_x = 0.34$ and $R_{ZJ} = 0.36$. Similarly, the $\omega = 19^\circ$ single-layer reconstruction proposed by Miller and Haneman²⁴ on the basis of oxygen spin-resonance data yielded $R_x = 0.27$ and $R_{ZJ} = 0.30$, comparable to the unreconstructed structure but significantly less satisfactory than the best-fit structures.

None of the structures in the vicinity of those given in rows (c)–(e) of Table I could be improved by the addition of second-layer reconstructions. This result may be a direct consequence of the fact that the ELEED data were acquired at room temperature. Since the energies of the second layer reconstructions are thought to lie in the range²⁶ $0.03 < E_2 < 0.05$ eV and at room temperature $\kappa T = 0.025$ eV, it is quite possible that thermal lattice vibrations have destabilized the second-layer distortions of GaP(110) relative to a low-temperature two-layer-relaxation structure analogous to those of GaAs(110),^{1,2} InSb(110),^{3,4} and InP(110).^{5,6} For ELEED intensities measured at 300 K, however, imposition of a second-layer shear analogous to those in GaAs, InSb, and InP consistently raises the calculated R factors for GaP(110) by $\Delta R_x \sim 0.03$ for each 0.1 Å of second-layer shear. Consequently, we have no reason to expect such reconstructions, although using Eq. (4) we cannot positively rule out as much as about 0.13 Å of second-layer shear.

Similarly, all reductions in the relaxations parallel to the surface of the top layer Ga or P relative to the bond-rotated structures increased both R_x and R_{ZJ} . Therefore, “rotational relaxation” model rather than a “bond-relaxation” model is clearly indicat-

ed by our analysis.

Finally, in order to examine the consequences of thermally induced lattice vibrations on the calculated ELEED intensities we utilized the values of $u^2(T)$ for both Ga and P extracted from the measured temperature dependence of x-ray Laue spots from GaP.¹¹ The computations were described in Sec. III and are shown in parts (e) of Figs. 6–14 for the minimum- R_x structure. The calculated intensities in parts (e) were multiplied by a factor of about 2 relative to those obtained for a rigid lattice and shown in parts (d) of the same figures. It is evident from the figures that this factor-of-2 suppression of the intensities from the vibrating relative to the rigid lattice is essentially the only significant effect of (*bulk*) lattice vibrations. Moreover, the R factors decrease by $\Delta R \sim 0.01$ for the vibrating relative to the rigid lattice for all of the structures near the optimal ones specified in Table I. Therefore the inclusion of bulk lattice vibrations into the analysis does not modify the results of our rigid-lattice structure analysis even though lattice vibrations near the surface might well suppress the second-layer reconstructions at higher (e.g., $T = 300$ K) temperatures.

VI. SYNOPSIS

Analysis of ELEED intensities from GaP(110) measured at $T = 300$ K leads to the selection of the best-fit surface structures as being single-layer rotational relaxation structures characterized by $\omega = 25^\circ \pm 3^\circ$ and a 0.1 ± 0.05 Å contraction of the uppermost layer spacing. An analysis of the accuracy of the structure analysis procedure reveals that these structures are *significantly better* than both the unreconstructed and all previously proposed^{24,25} structures by virtue of variations in R_x which lie well outside the uncertainties ($\Delta R_x = 0.04$) inherent in calculations of this quantity for a fixed data set and a given structural model.

ACKNOWLEDGMENTS

The authors are indebted to L. J. Kennedy for assistance and to M. D. Tabak for generous support of this work. This research also was supported in part by the Office of Naval Research Grant No. N00014-75-C-0394.

- ¹C. B. Duke, R. J. Meyer, A. Paton, P. Mark, A. Kahn, E. So, and J. L. Yeh, *J. Vac. Sci. Technol.* **16**, 1252 (1979).
- ²R. J. Meyer, C. B. Duke, A. Paton, A. Kahn, E. So, J. L. Yeh, and P. Mark, *Phys. Rev. B* **19**, 5194 (1979).
- ³C. B. Duke, R. J. Meyer, A. Paton, J. L. Yeh, J. C. Tsang, A. Kahn, and P. Mark, *J. Vac. Sci. Technol.* **17**, 501 (1979).
- ⁴R. J. Meyer, C. B. Duke, A. Paton, J. L. Yeh, J. C. Tsang, A. Kahn, and P. Mark, *Phys. Rev. B* **21**, 4740 (1980).
- ⁵C. B. Duke, R. J. Meyer, and P. Mark, *J. Vac. Sci. Technol.* **17**, 971 (1980).
- ⁶R. J. Meyer, C. B. Duke, A. Paton, J. C. Tsang, J. L. Yeh, A. Kahn, and P. Mark, *Phys. Rev. B* **22**, 6171 (1980).
- ⁷C. B. Duke, R. J. Meyer, A. Paton, P. Mark, E. So, and J. L. Yeh, *J. Vac. Sci. Technol.* **16**, 647 (1979).
- ⁸R. J. Meyer, C. B. Duke, A. Paton, E. So, J. L. Yeh, A. Kahn, and P. Mark, *Phys. Rev. B* **22**, 2875 (1980).
- ⁹R. J. Meyer, C. B. Duke, and A. Paton, *Surf. Sci.* **97**, 512 (1980).
- ¹⁰C. B. Duke, *Adv. Chem. Phys.* **27**, 1 (1974); in *Dynamic Aspects of Surface Physics; Proceedings of the International School of Physics Enrico Fermi*, edited by F. O. Goodman (Editrice Compositori, Bologna, 1974), pp. 99–173.
- ¹¹M. G. Shumskii, V. T. Bublik, S. S. Gorelik, and M. A. Gurevich, *Kristallografiya* **16**, 779 (1971) [*Sov. Phys. Crystallogr.* **16**, 674 (1972)].
- ¹²J. F. Vetelino, S. P. Gaur, and S. S. Mitra, *Phys. Rev. B* **5**, 2360 (1972).
- ¹³R. W. G. Wyckoff, *Crystal Structures* (Wiley, New York, 1963), Vol. I, pp. 108–111.
- ¹⁴J. C. Phillips, *Rev. Mod. Phys.* **42**, 317 (1970).
- ¹⁵C. B. Duke, N. O. Lipari, and U. Landman, *Phys. Rev. B* **8**, 2454 (1973).
- ¹⁶J. C. Slater, *Phys. Rev.* **18**, 385 (1951).
- ¹⁷S. Hara, *J. Phys. Soc. Jpn.* **22**, 710 (1967).
- ¹⁸C. B. Duke and C. W. Tucker, Jr., *Surf. Sci.* **15**, 231 (1969).
- ¹⁹E. Zanazzi and F. Jona, *Surface Sci.* **62**, 61 (1977).
- ²⁰D. W. Jepson, P. M. Marcus, and F. Jona, *Phys. Rev. B* **5**, 3933 (1972).
- ²¹Ignatiev, F. Jona, M. Debe, D. E. Johnson, S. J. White, and D. P. Woodruff, *J. Phys. C* **10**, 1109 (1977).
- ²²C. B. Duke, R. J. Meyer, A. Paton, A. Kahn, J. Carel-ij, and J. Yeh, *J. Vac. Sci. Technol.* **18**, 866 (1981).
- ²³H. D. Shih, F. Jona, U. Bardi, and P. M. Marcus, *J. Phys. C* **13**, 3801 (1980).
- ²⁴D. J. Miller and D. Haneman, *Surface Sci.* **82**, 102 (1979).
- ²⁵B. W. Lee, R. K. Ni, and N. Masud, *Abstracts of the Eighth Annual Conference on the Physics of Compound Semiconductors* (Naval Research Laboratory, Washington, D. C. 1981), paper 2.
- ²⁶D. J. Chadi, *Phys. Rev. B* **19**, 2074 (1979).